Journal of Engineering Mathematics (2006) 56: 79–99
DOI 10.1007/s10665-006-9041-6

On some approximate methods for the tensile instabilities of thin annular plates

CIPRIAN D. COMAN and DAVID M. HAUGHTON
Department of Mathematics, University of Glasgow, University Gardens, Glasgow G12 8QW, Scotland, UK (cdc@maths.gla.ac.uk)

Received 31 August 2005; accepted in revised form 9 February 2006 / Published online: 28 June 2006

Abstract. A thin annular plate is subjected to a uniform tensile field at its inner edge which leads to compressive circumferential stresses. When the intensity of the applied field is strong enough, elastic buckling occurs circumferentially, leading to a *wrinkling pattern*. Using a linear non-homogeneous pre-bifurcation state, the linearised eigenvalue problem describing this instability is cast as a fourth-order linear differential equation with variable coefficients. This problem is investigated numerically and it is shown that the simple application of the Galerkin technique reported in the literature leads to gross errors in the corresponding approximations. Several novel mathematical features of the eigenvalue problem are included as well.

Key words: annular plates, buckling, Galerkin technique, Rayleigh quotient, wrinkling

1. Introduction

Historically, the understanding of elastic instabilities in solids subjected to compressive loads has always played a pivotal role in the efficient design of slender mechanical structures [1]. By far, the most studied case discussed in the literature pertains to the situation in which a structure is subjected to a global *compressive* load. In this scenario, as the load is increased through some critical value, the structure passes from its natural, undistorted configuration, to an arbitrarily close equilibrium shape which is qualitatively different from the original one; this is the so-called *buckled state*. From a mathematical point of view, buckling represents a typical bifurcation phenomenon on which many of the modern tools of bifurcation theory can be brought to bear [2].

Much less attention has been paid to the occurrence of elastic instabilities when a given structure is subjected to *global tensile loads*, mostly because such problems are not as prevalent as the classical buckling phenomenon. Nevertheless, there are a number of practical applications in which such problems crop up, and they have been the subject of several investigations which we briefly review below.

The buckling of an annular plate subjected to tensile stress along its inner edge has attracted considerable interest due to its relevance in the manufacturing process of forming a flat sheet metal blank into a cylindrical cup-shaped product, a mechanical operation known as *deep drawing*; a full account of this theory can be found in [3, pp. 292–315] and [4, pp. 328–347], which contain additional pointers to the literature. This process is characterised by the use of a cylindrical punch and an annular die, the sheet being drawn radially inwards over the die profile by the advancing punch. The stress/strain distribution in such an operation is very complex and one has to rely on introducing reasonable simplifications in the mathematical modelling. In understanding the possible instabilities of deep drawing, a

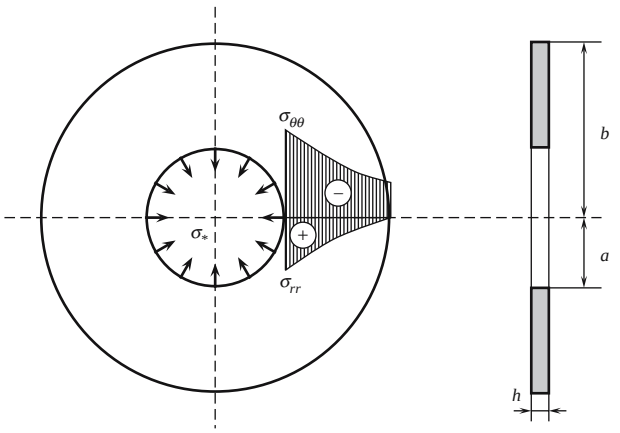

Figure 1. The geometry of the annular plate subjected to a uniform tension field σ_* on its inner boundary and tension-free on the outer one. The variable hoop ($\sigma_{\theta\theta}$) and radial (σ_{rr}) stresses are compressive and, respectively, tensile, *throughout* the plate.

widely accepted approximation consists in considering an annular plate subjected to a uniform tension field along its inner edge (*cf*. [5–7]). Although the global loading is stabilising with respect to the buckling instability, the presence of a hole in the plate leads to an interesting pre-buckling stress distribution. The hoop stress, $\sigma_{\theta\theta}$, is compressive, reaches its maximum amplitude on the inner edge of the plate, and is directly proportional to the applied stress σ_* (see Figure 1). When this applied load reaches a critical value, the plate undergoes elastic buckling circumferentially, a phenomenon referred to as *elastic wrinkling* in the literature.

Geckler [8] provided a first approximate study of this problem by considering the plastic regime, and his work was then followed by many others (*cf*. [3, pp. 345–347]). A considerable improvement of his results was achieved by Senior [5] who made several assumptions regarding the deflected form of the plate and then evaluated the component quantities of the potential energy related to a small deformation. By equating the total energy tending to restore equilibrium to that due to forces displacing it, he found the critical stability conditions; this line of inquiry resulted in a set of lower and upper bounds for both the critical stress and the number of circumferential wrinkles. Mansfield [9] dealt with the elastic buckling of an annular plate subjected to either compression or tension on its inner boundary. His approach was based on the classical buckling equation of annular plates (for example, see [10, pp. 173–178]) together with a simplified pre-buckling state that led to closed-form solutions for his problem. As already noted by Yu and Johnson [7], his solution is valid, strictly speaking, only for plates with an infinite outer radius. A systematic analysis of both the elastic and plastic instabilities related to annular plates in tension was undertaken by Yu and co-workers [6, 7]. However, that work is open to some criticism that we shall present in detail over the next sections.

More recently, the wrinkle formation in thin plates (or membranes) has been the object of several interesting studies. Friedl *et al*. [11] have showed numerically that buckling due to global tension can occur as a result of special boundary conditions. For the case of a thin rectangular plate loaded on two opposite sides, they showed that these conditions provide a constraint for the lateral contraction due to the Poisson's effect, whose role is to produce lateral compressive stresses away from the boundary. This results in a sequence of wrinkles parallel to the direction of applied tension. Cerda and Mahadevan [12] presented a heuristic analysis of wrinkling in thin elastic sheets valid far in the nonlinear regime, dealing mainly with various scaling laws for the wavelength of the wrinkles and their amplitude. In

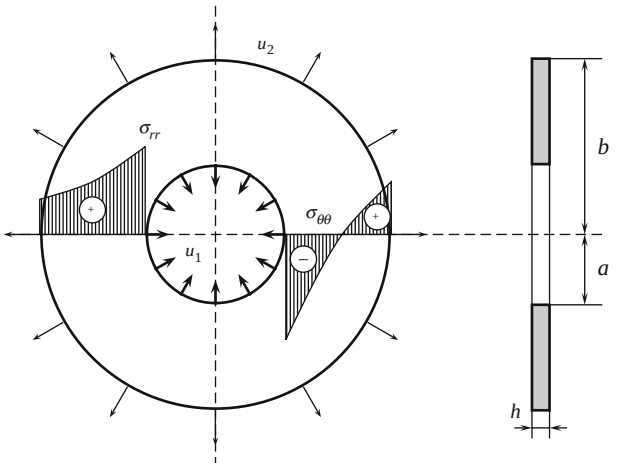

Figure 2. An annular plate subjected to uniform displacement fields on its boundaries. In this case the hoop stress $\sigma_{\theta\theta}$ changes from *compressive*, near the inner boundary, to *tensile*, in the complementary region.

a follow-up work [13], Cerda discussed some biomedical applications regarding the effect of background tension of the skin on the formation of wrinkles around circular scars.

The mechanics of wrinkle formation has also found novel applications in cell biomechanics [14, 15], as it provides insight into living cell locomotion. Roughly speaking, the quantitative analysis of wrinkled patterns produced by cells crawling on elastic membranes gives an indication of the force applied by the cell cytoskeleton. Géminard *et al*. [16] have provided an experimental and numerical study of a model that mimics this situation. They employed the Donnell–von Kármán equations involving nonlinear kinematics, and used a linear pre-buckling state for a pre-stressed annular plate subjected to a uniform displacement field along its inner boundary. In Figure 2 the initial stretching of the plate is due to the (fixed) displacement field u_2 imposed on the outer edge, while the loading is realised by applying the radial displacement field u_1. The particular type of loading adopted yields a hoop stress distributions that is compressive in a concentric region adjacent to the inner edge, while in the remaining part of the plate this stress is tensile. The result is a wrinkling pattern localised near the inner edge, and, as shown by Coman and Haughton in [17], several features of this problem can be understood by looking at the linearised bifurcation equation.

Although only remotely related to the present work, we note here the original contribution [18] in which Gilabert *at al*. established numerically and experimentally the existence of complex spatial patterns around defects such as holes or cracks in a thin stretched plate. The "Maltese cross" buckling pattern reported in that reference is triggered by a local compressive stress induced by the presence of the defect, and is strongly dependent on the thickness of the plate, a situation similar to that depicted in Figure 2.

Our main aim in this work is to revisit the elastic wrinkling instabilities discussed in [6, 7] and provide an assessment of the approximations reported therein. To this end, the paper is laid out as follows. In order to make the work in this paper reasonably self-contained, in Section 2 we formulate the non-homogeneous eigenvalue problem that governs the elastic instabilities of the annular plate discussed above. We then proceed in Section 3 to embark on a numerical investigation regarding the dependence of the lowest critical eigenvalue on various quantities of interest, and perform a comparison with similar results in the literature. The difficulties experienced by the approximate techniques for this problem are interpreted in light

of the corresponding Rayleigh quotient, and the paper ends with a few remarks and some open issues to be considered in future research.

2. Problem statement

We consider a thin annular plate of inner radius a, outer radius b, and thickness $h (h/b \ll 1)$, corresponding to the situation shown in Figure 1. As usually, a cylindrical system of coordinates (r, θ, z) is used to define various quantities of interest associated to this problem. Displacement components in the r, θ, and z directions, respectively, are denoted by u_r, u_θ, and w. The internal strains of interest are defined according to

$$\varepsilon_{rr} = \frac{\partial u_r}{\partial r}, \qquad \varepsilon_{\theta\theta} = \frac{1}{r}\left(\frac{\partial u_\theta}{\partial \theta} + u_r\right), \qquad \varepsilon_{r\theta} = \frac{1}{2}\left(\frac{1}{r}\frac{\partial u_r}{\partial \theta} + \frac{\partial u_\theta}{\partial r} - \frac{u_\theta}{r}\right), \tag{1}$$

and the corresponding stresses are assumed to obey the classical Hooke's Law

$$\sigma_{ij} = 2\mu\varepsilon_{ij} + \lambda(\varepsilon_{rr} + \varepsilon_{\theta\theta})\delta_{ij}, \quad i, j \in \{r, \theta\}, \tag{2}$$

where μ and λ are the Lamé constants and δ_{ij} is the usual Kronecker delta.

The linear pre-buckling state of stress in the annular plate is determined by solving the system of equilibrium equations of plane stress elasticity (see [19, pp. 260–267])

$$\frac{\partial \sigma_{rr}}{\partial r} + \frac{1}{r}\frac{\partial \sigma_{r\theta}}{\partial \theta} + \frac{1}{r}(\sigma_{rr} - \sigma_{\theta\theta}) = 0, \tag{3a}$$

$$\frac{\partial \sigma_{r\theta}}{\partial r} + \frac{1}{r}\frac{\partial \sigma_{\theta\theta}}{\partial \theta} + \frac{2}{r}\sigma_{r\theta} = 0, \tag{3b}$$

which must be supplemented with an appropriate set of boundary conditions. In this paper we shall assume that the pre-buckling state is axisymmetric, *i.e.*, $u_r = U(r)$ and $u_\theta \equiv 0$, for some function U, while the boundary conditions are taken to be

$$\begin{cases} \sigma_{rr}(r) = \sigma_* \\ \sigma_{r\theta}(r) = 0, \end{cases} \quad \text{for } r = a, \qquad \text{and} \qquad \begin{cases} \sigma_{rr}(r) = 0 \\ \sigma_{r\theta}(r) = 0, \end{cases} \quad \text{for } r = b. \tag{4}$$

After some simple manipulations, one finds that the *variable* pre-buckling stress distribution in the plate is given by

$$\sigma_{rr}^{(0)} = \frac{\sigma_* a^2 b^2}{b^2 - a^2}\left(\frac{1}{r^2} - \frac{1}{b^2}\right) \qquad \text{and} \qquad \sigma_{\theta\theta}^{(0)} = -\frac{\sigma_* a^2 b^2}{b^2 - a^2}\left(\frac{1}{r^2} + \frac{1}{b^2}\right), \tag{5}$$

where the superscript 0 has been used to indicate that these quantities represent pre-bifurcation fields.

The linearised bifurcation equation governing the instability of the annular plate can now be given as (see [10 pp. 173–176], [20 pp. 89–91], [21 pp. 234–241] for details)

$$D\nabla^4 w - h\left[\sigma_{rr}^{(0)}\frac{\partial^2 w}{\partial r^2} + \sigma_{\theta\theta}^{(0)}\frac{1}{r}\left(\frac{\partial w}{\partial r} + \frac{1}{r}\frac{\partial^2 w}{\partial \theta^2}\right)\right] = 0, \tag{6}$$

where $D = Eh^3/12(1-\nu^2)$ is the bending stiffness of the plate, ν is the Poisson's ratio, and E is Young's modulus. Here

$$\nabla^2 := \frac{\partial^2}{\partial r^2} + \frac{1}{r}\frac{\partial}{\partial r} + \frac{1}{r^2}\frac{\partial^2}{\partial \theta^2},$$

is the Laplacian in polar coordinates, and $\nabla^4(\bullet) \equiv \nabla^2\left(\nabla^2(\bullet)\right)$.

In general, the method of separation of variables does not lead to closed form solutions for the non-homogeneous bifurcation equation unless it is assumed *a priori* that the buckling solution has axial symmetry; however, this is an unreasonable assumption as transpires from direct numerical integration. Mansfield [9] ignored the $1/b^2$ terms in (5), and this led him to an integrable case which allowed a simple analytical solution of (6).

Substituting (5) in (6), and rescaling the independent co-ordinate according to $\rho := r/b$, the bifurcation equation becomes

$$\mathcal{L}_0[w] - \Lambda^2 \left(\frac{1}{\rho^2} \mathcal{L}_1^-[w] - \mathcal{L}_1^+[w] \right) = 0, \tag{7}$$

where we have introduced the following differential operators

$$\mathcal{L}_1^{\pm} := \frac{\partial^2}{\partial \rho^2} \pm \frac{1}{\rho} \frac{\partial}{\partial \rho} \pm \frac{1}{\rho^2} \frac{\partial^2}{\partial \theta^2}, \qquad \mathcal{L}_0 := \left(\frac{\partial^2}{\partial \rho^2} + \frac{1}{\rho} \frac{\partial}{\partial \rho} + \frac{1}{\rho^2} \frac{\partial^2}{\partial \theta^2} \right)^2,$$

and

$$\Lambda^2 := \frac{a^2 b^2}{b^2 - a^2} \left(\frac{h}{D} \right) \sigma_* \tag{8}$$

is the unknown non-dimensional eigenvalue; for later purposes, we set $\eta := a/b$. Next, we look for solutions of the bifurcation equation of the form

$$w(\rho, \theta) = W(\rho) \cos(n\theta), \tag{9}$$

where $n \in \mathbb{N}$ is the mode number (the number of identical circumferential wrinkles). On making use of this form of solution, we find

$$\mathcal{L}_0[w] = \left\{ W'''' + \frac{2}{\rho} W''' - \left(\frac{2n^2+1}{\rho^2} \right) W'' + \left(\frac{2n^2+1}{\rho^3} \right) W' + \left[\frac{n^2(n^2-4)}{\rho^4} \right] W \right\} \cos(n\theta),$$

$$\mathcal{L}_1^{\pm}[w] = \left[W'' \pm \frac{1}{\rho} W' \mp \frac{n^2}{\rho^2} W \right] \cos(n\theta),$$

and, after some simple algebra, the amplitude $W \equiv W(\rho)$ of the normal-mode solution can be shown to satisfy the following differential equation with variable coefficients

$$W'''' + \mathcal{A}(\rho;\, \Lambda) W''' + \mathcal{B}(\rho;\, \Lambda) W'' + \mathcal{C}(\rho;\, \Lambda) W' + \mathcal{D}(\rho;\, \Lambda) W = 0, \quad \eta < \rho < 1, \tag{10}$$

where

$$\mathcal{A}(\rho;\, \Lambda) := \frac{2}{\rho}, \qquad \mathcal{B}(\rho;\, \Lambda) := -\left[\frac{2n^2+1}{\rho^2} + \Lambda^2 \left(-1 + \frac{1}{\rho^2} \right) \right],$$

$$\mathcal{C}(\rho;\, \Lambda) := \frac{1}{\rho} \left[\frac{2n^2+1}{\rho^2} + \Lambda^2 \left(1 + \frac{1}{\rho^2} \right) \right], \quad \mathcal{D}(\rho;\, \Lambda) := \frac{n^2}{\rho^2} \left[\frac{n^2-4}{\rho^2} - \Lambda^2 \left(1 + \frac{1}{\rho^2} \right) \right].$$

Equation (10) must be supplemented with appropriate boundary conditions, which can be obtained by using the separation of variable method employed above. For the deep-drawing processes discussed in [6, 7], the inner edge ($\rho = \eta$) was taken to be simply supported, while the outer edge was assumed to be free. This results in the following set of conditions for $W(\rho)$ (see [6, 9], [21, pp. 236–237] for more details)

$$W = 0, \qquad \text{for} \quad \rho = \eta, \tag{11a}$$

$$W'' + \frac{\nu}{\rho} W' - \frac{\nu n^2}{\rho^2} W = 0, \qquad \text{for} \quad \rho = \eta,\ 1, \tag{11b}$$

$$W''' + \frac{1}{\rho} W'' - \left[\frac{1 + (2-\nu)n^2}{\rho^2}\right] W' + \left[\frac{(3-\nu)n^2}{\rho^3}\right] W = 0 \quad \text{for} \quad \rho = 1, \tag{11c}$$

irrespective of the pre-buckling state.

For the sake of completeness we shall dwell a little further on these four boundary conditions. It is well known that the variational approach for the Kirchhoff theory of classical linear elastic plates leads to the following two sets of natural and kinematic boundary conditions,

$$\text{either} \quad M_r = 0 \quad \text{or} \quad \frac{\partial w}{\partial r} \quad \text{is prescribed}, \tag{12a}$$

$$\text{either} \quad Q_r + \frac{1}{r}\frac{\partial M_{r\theta}}{\partial \theta} = 0 \quad \text{or} \quad w \quad \text{is prescribed}, \tag{12b}$$

where M_r, $M_{r\theta}$, and Q_r represent the bending moments and, respectively, the shear force associated with the polar coordinates indicated (see [22, pp. 297–298]). For the simply supported edge ($\rho = \eta$) we have used the kinematic boundary condition given in (12b) and the natural one in (12a). For the free edge ($\rho = 1$) there are no kinematic boundary conditions applicable and hence we should enforce both natural boundary conditions in (12). These can then be conveniently expressed in terms of the transverse displacement alone, using (9) and the classical formulae for plates [10, pp. 160–161], [20, pp. 208–209]

$$M_r = -D\left(\frac{\partial^2 w}{\partial r^2} + \frac{\nu}{r}\frac{\partial w}{\partial r} + \frac{\nu}{r^2}\frac{\partial^2 w}{\partial \theta^2}\right),$$

$$M_{r\theta} = -D(1-\nu)\left(\frac{1}{r}\frac{\partial^2 w}{\partial r \partial \theta} - \frac{1}{r^2}\frac{\partial w}{\partial \theta}\right),$$

$$Q_r = -D\frac{\partial}{\partial r}\left(\frac{\partial^2 w}{\partial r^2} + \frac{1}{r}\frac{\partial w}{\partial r} + \frac{1}{r^2}\frac{\partial^2 w}{\partial \theta^2}\right),$$

thus leading to the boundary conditions recorded in (11). We note in passing that the rescaling adopted above seems to have eliminated any small parameter in equations (10) and (11). The material constant ν may have any value between 0 and 1/2, but usually it is about 0·3 for mild steel; in general, variations in ν affect the solutions of structural mechanics problems very little. We therefore chose a convenient fixed value, equal to 0·3, in our numerical calculations. The only essential parameters that remain in (10) and (11) are the ratio $a/b \equiv \eta$, the mode number n, and the unknown eigenvalue Λ.

3. A numerical study

We perform numerical simulations of the bifurcation equation (10) that describes the tensile instabilities of the annular plate considered in Section 2. Our main objective here is to discuss the dependence of Λ on a/b and n, and to show that some of the previous approximate solutions reported in the literature [6] are rather unsatisfactory when compared with their counterparts obtained by numerical integration. To this end, the bifurcation equation is cast in the standard form

$$\frac{\mathrm{d}\mathbf{w}}{\mathrm{d}\rho} = \mathbf{A}(\rho;\ \Lambda,\ n)\mathbf{w}, \quad \eta < \rho < 1 \tag{13}$$

by introducing the usual dependent variables

$$w_1(\rho) := W(\rho), \qquad w_2(\rho) := W'(\rho), \qquad w_3(\rho) := W''(\rho), \qquad w_4(\rho) := W'''(\rho),$$

and then letting $\mathbf{w} := (w_1, w_2, w_3, w_4)^T$. The expression of the matrix $\mathbf{A} \in M_{4\times4}(\mathbb{R})$ can be found by carrying out the above substitutions. Also, the boundary conditions (11) can be written in vector form as

$$\mathbf{B}_1(\rho;\ n)\mathbf{w} = \mathbf{0} \qquad \text{for} \quad \rho = \eta, \tag{14a}$$

$$\mathbf{B}_2(\rho;\ n)\mathbf{w} = \mathbf{0} \qquad \text{for} \quad \rho = 1, \tag{14b}$$

for some appropriate matrices $\mathbf{B}_1,\ \mathbf{B}_2 \in M_{2\times4}(\mathbb{R})$.

Next, the compound matrix method [23, pp. 311–317] is used to integrate numerically the boundary value problem (13) and (14); this is a well tested technique which performs particularly well in calculating the response curves for a range of problems in solid mechanics [24–26]. A detailed account regarding the implementation of this method for a similar problem was given by one of us in [24], and the reader is referred to that paper for more details. We have also double checked our results using the boundary value solver AUTO97 [27] and the results were found to be identical to within the numerical errors associated with the calculations.

By analogy with the classical Sturm-Liouville problems for ordinary differential equations [28, pp. 42–78], one would expect that for any given $n \geq 0$ and $\eta \equiv a/b \in (0,\ 1)$, the boundary value problem (10) and (11) has a set of real eigenvalues, say $\Lambda_p(\eta,\ n)$, where $p = 1,\ 2,\ \ldots$, ordered according to increasing order of magnitude. However, since we are dealing with a generalised eigenvalue problem here, it is not necessarily true that these eigenvalues exist for all stated values of η and n, nor that $\Lambda_p \to \infty$ as $p \to \infty$. Indeed, when $n = 0$ or $n = 1$, our numerical searches revealed that there are no positive real eigenvalues. For all practical purposes, it is the lowest positive eigenvalue, Λ_1, which is of interest, and we shall focus our attention on this quantity; for simplicity of notation we shall refer to it as Λ. Since according to (8) the expression of Λ depends explicitly on a/b, it is useful to also use $\Lambda_* := \sigma_* b^2 h/D$ as an alternative choice for the eigenvalues of (13) and (14); this will be subject to the same restrictions as stated above.

In Figure 3 we illustrate the dependence of the first eigenvalue on the ratio a/b and the mode number n. The plot shown consists of a series of curves, denoted by C_n, that describe the dependence of Λ on η for each $n = 2,\ \ldots,\ 13$; the two arrows indicate the increasing direction of the number of wrinkles, n. For plates for which $a \ll b - a$, corresponding to those with a small inner radius, the critical mode number is $n = 2$, and the eigenvalues are given by the lower part of C_2; this is in qualitative agreement with Mansfield's results for infinite annular plates [9]. The critical mode number changes to $n = 3$ when $a/b = 0{\cdot}406$, and this value of n continues to be relevant until $a/b = 0{\cdot}62$, when the critical number of wrinkles is increased by 1 and the eigenvalues start following the curve C_4. This switching process between the response curves continues *ad infinitum*, and as $a/b \to 1$ the crossing frequency of the curves C_n and C_{n+1} increases, as it can be clearly seen in Figure 3. Also, $\Lambda \to \infty$ in that limit, although this is not obvious from the recorded plots but it was confirmed by our careful numerical simulations, and it is discussed further in the next section. The case of interest in a deep-drawing operation corresponds to the situation when $b - a \ll b$ in which the width of the annular region is much smaller than the outer radius of the plate. Our numerical experiments and the results recorded in Figure 3 show that as the value of a/b increases (getting closer

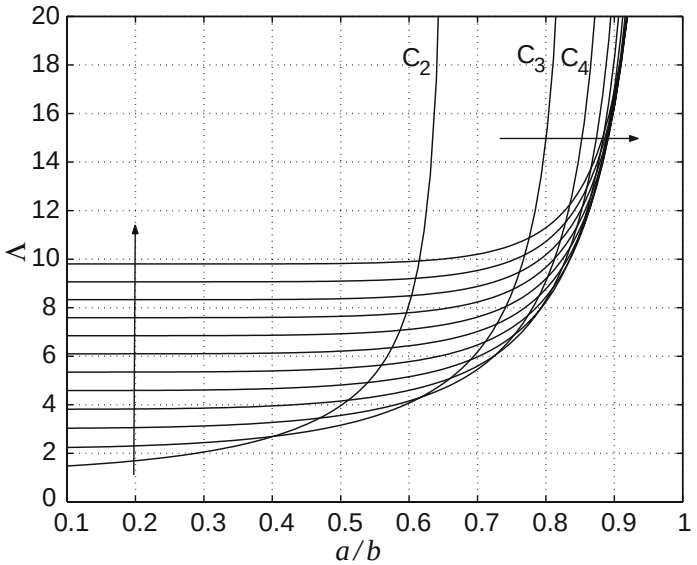

Figure 3. The response curves $\Lambda = \Lambda(\eta, n)$ for the buckling equation (10) corresponding to $n = 2, \ldots, 13$; the arrows indicate the direction of increasing n.

to 1) the critical mode number n cannot be predicted accurately because of its extreme sensitivity with respect to this ratio.

It is important to establish the limit of validity for the occurrence of the elastic instability discussed above. For the sake of completeness, next, we follow [7] and record such a result in order to provide some orientative guidance for the interpretation of Figure 3. A detailed quantitative assessment between the plastic and the elastic wrinkling instabilities is beyond the scope of this paper. Most investigators have focused exclusively on the case when wrinkling occurs in the plastic regime [3, pp. 311–315], [4, pp. 343–345], [5, 8, 29], although if elastic wrinkling is triggered before plastic yielding takes place, this results in an unsatisfactory manufacturing operation. It is a well known fact [4, pp. 318–321] that under the given type of loading and particular geometry adopted in this paper, plastic yielding occurs first on the inner edge, $r = a$. By letting σ_Y denote the yield stress of the material, the corresponding Tresca yield criterion is

$$\sigma_{rr}^{(0)} - \sigma_{\theta\theta}^{(0)} = \sigma_Y \qquad \text{for} \quad r = a.$$

Using (5), we find that

$$\sigma_*^{(p)} = \sigma_Y \left(\frac{1-\eta^2}{2} \right), \tag{15}$$

where $\sigma_*^{(p)}$ is the critical value of σ_* for which the material enters the plastic range. On the other hand, the definition of Λ allows us to express σ_* in terms of this quantity, according to

$$\sigma_* = \frac{D\Lambda^2}{hb^2} \left(\frac{1-\eta^2}{\eta^2} \right). \tag{16}$$

The range of validity for our elastic analysis is obtained by enforcing $\sigma_* \leq \sigma_*^{(p)}$, which can be re-arranged in a more convenient form as

$$\frac{b-a}{h} \geq \frac{\Lambda(1-\eta)}{\eta\sqrt{6(1-\nu^2)}}\sqrt{\frac{E}{\sigma_Y}}\,. \tag{17}$$

The interpretation of this formula is straightforward. For a given annular plate, the constant materials E and σ_Y are assumed to be available, and by specifying the ratio $a/b \equiv \eta$ the value of Λ can be obtained from Figure 3. In consequence, (17) provides a lower bound for the width of the flange, $b-a$, in terms of the thickness of the plate, h.

In references [6, 7], Yu and his co-workers proposed some approximate results for the eigenvalues of the bifurcation equation (7) using the method of separation of variables. A Galerkin method à la Kantorovich was proposed in [6] in an attempt to improve an earlier solution based on a variational formulation of (7); the solution in this case was obtained with the help of the Rayleigh–Ritz approach via a simple choice of test function. However, these authors did not compare their approximations against the full numerical solution reported herein, and thus the validity of their results has remained unquestioned so far.

The comparison of our results with those corresponding to the elastic wrinkling problem in [6] are shown in Figures 4 and 5, where the continuous lines represent the results of this investigation and the dashed line the Galerkin approximations. In both plots we have used the original scaling for eigenvalues employed by Yu and Zhang, and we have used the same choice of values for n as in their work. The two arrows, the continuous and the dashed ones, indicate the direction of increasing n for the two sets of curves. It turns out that the Galerkin solution provides a conservative estimate for the eigenvalues Λ_*, but it is in disagreement with the numerical solution. The Galerkin approximation used by the above authors required a choice of trial function identically satisfying the boundary conditions (11a) and (11b), while the natural boundary condition (11c) was ignored. However, the expression of this test function suggested in [6] is wrong, as the indicial equation for the differential equation associated with (11b) has a positive discriminant, and thus its solutions are of exponential type. We have used the correct expression for the trial function in plotting the results in Figures 4 and 5. According to our numerical findings it seems that the critical stress σ_* does *not* decrease monotonically with increasing the inner radius $r=a$ when the outer radius $r=b$ is held constant, an important fact that is not captured by the approximate solution.

In the literature on plastic wrinkling, many authors have employed the additional condition $w(\rho, \theta) \geq 0$ for all $(\rho, \theta) \in [\eta, 1] \times (0, 2\pi]$, because the possible deformations of the die are assumed negligible in comparison to those experienced by the plate. This is not necessarily true for elastic wrinkling, as noted in [6], and a possible candidate for the separable variable solution (9) in the former case is, $w(\rho, \theta) = W(\rho)(1+\cos(n\theta))$. Thus, a natural question is, what is the difference between the critical values of Λ as predicted by the two different approaches? An elastic wrinkling stability analysis based on an energy method and using the additional positivity condition for the transverse displacement was undertaken in [7], where the kinematics adopted is similar to ours, and the prebuckling state is identical. According to [29], the critical loads reported in that reference are slightly lower than those obtained through alternative approaches and based on the same assumptions. We have compared the critical curves presented [7] with our numerical solutions, and these results are summarised in Figures 6 and 7; the arrows have the same meaning as in the previous two Figures already shown. As clearly shown in these plots, the onset of elastic wrinkling in our case (and in [6]) occurs much earlier than predicted in [7]. An individual comparison between the response curves for $n=4, 5, 6, 7$ is shown in Figure 7.

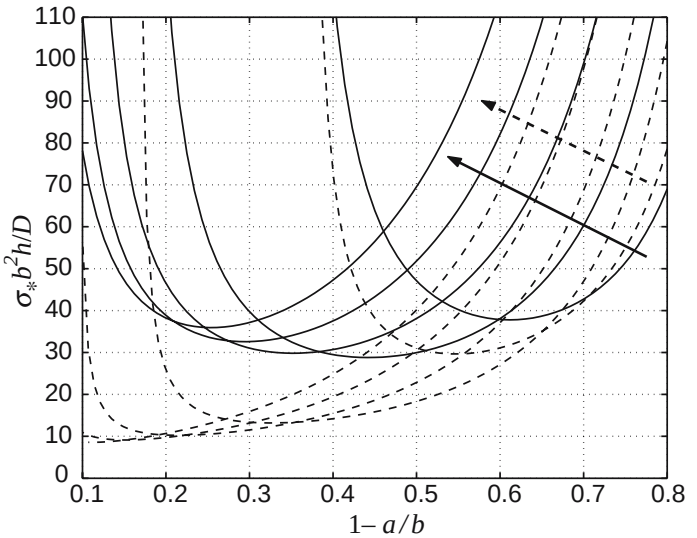

Figure 4. Comparisons between the response curves for the wrinkling instability of the annular plate for $n = 2, \ldots, 6$; the arrows indicate the direction of increasing n. The continuous curves show the numerical results of the present analysis, while the dashed ones are their Galerkin approximations as obtained by Yu and Zhang [6].

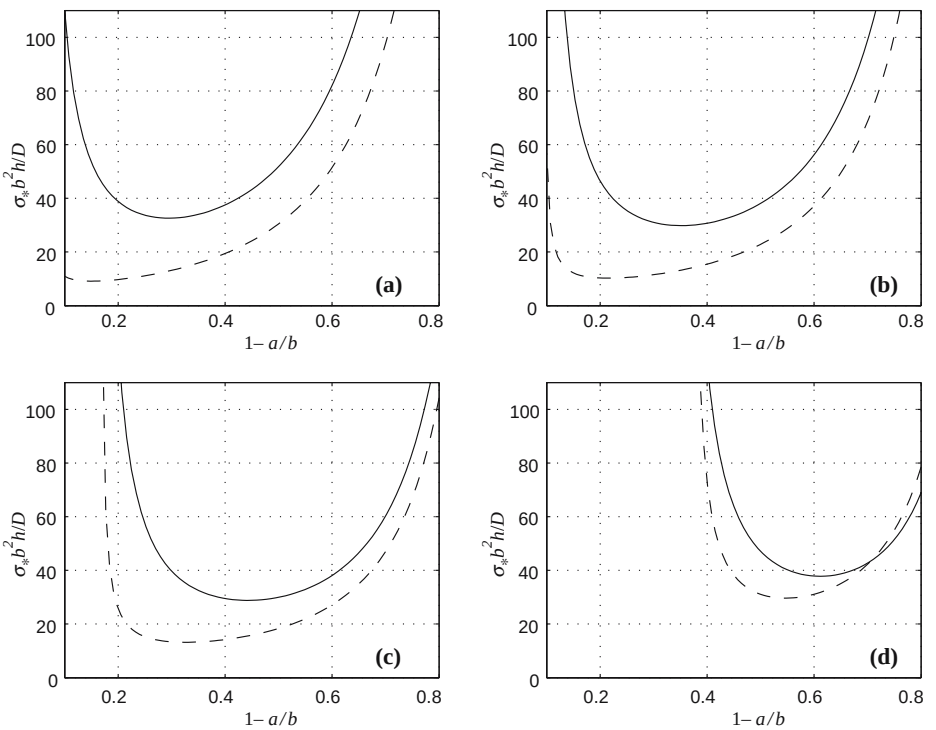

Figure 5. A closer look at Figure 4: comparisons between the numerics (continuous line) and the Galerkin approach (dashed line); $n = 5(a), n = 4(b), n = 3(c), n = 2(d)$.

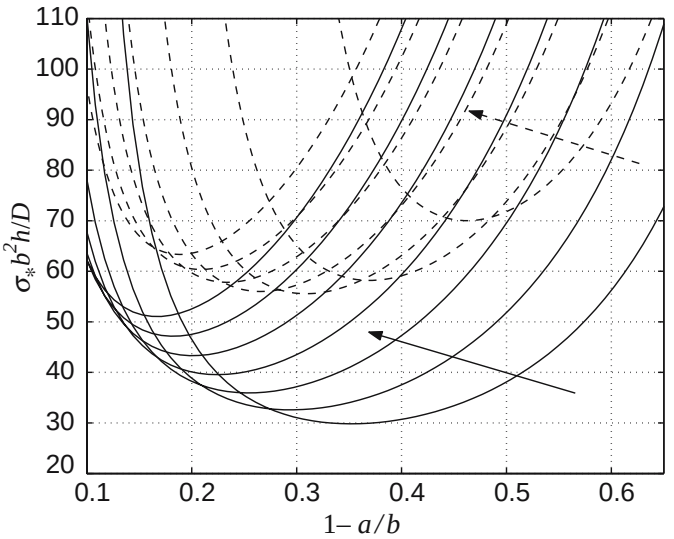

Figure 6. The response curves for the wrinkling instability of the annular plate for $n=4, \ldots, 10$; the arrows indicate the direction of increasing n. The continuous curves show our numerical results obtained from (7) with $w(\rho, \theta) = W(\rho)\cos(n\theta)$; the dashed lines are those given in [7] and based on an equivalent variational formulation of the same bifurcation equation but under the assumption that $w(\rho, \theta) = W(\rho)(1+\cos(n\theta))$.

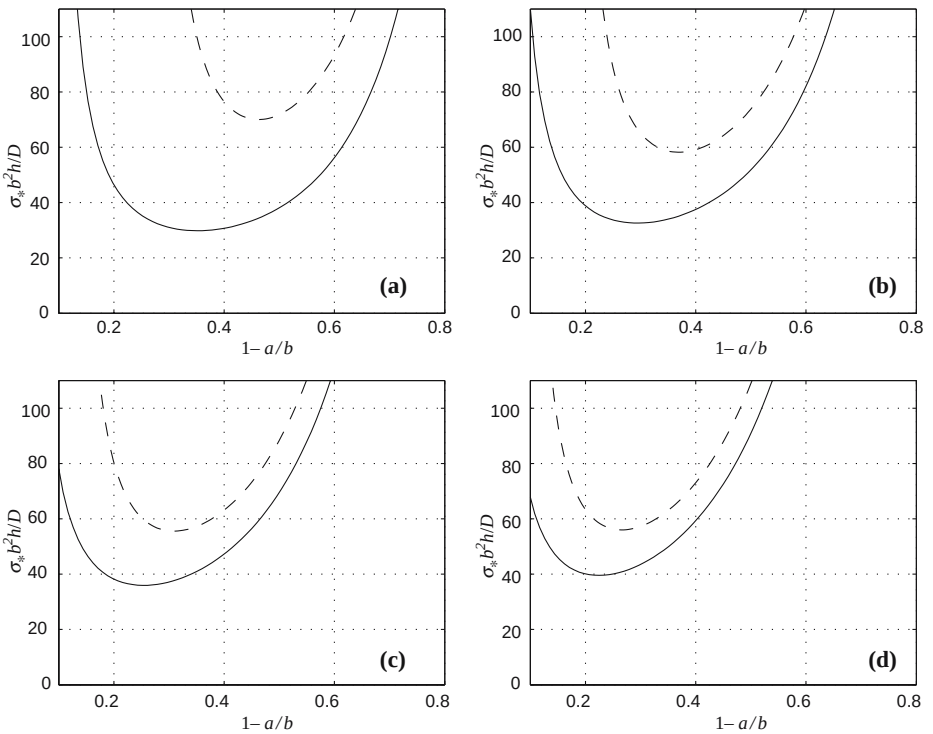

Figure 7. A closer look at Figure 6 (the same conventions apply): $n=4(a), n=5(b), n=6(c), n=7(d)$.

To summarise, the approximate Galerkin solution of Yu and Zhang can be regarded as a *lower* bound for the true eigenvalues of (10) and (11), although its practical relevance should be justly regarded with suspicion. Also, imposing the additional kinematic constraint $w \geq 0$ on the solutions of (7) results in much higher critical values for Λ.

4. Some approximations

To understand the reasons for the poor performance of the Galerkin method, we need to recast the eigenvalue problem (10)–(11) in a more suitable form

$$\mathcal{M}[W] = \Lambda^2 \mathcal{N}[W], \tag{18}$$

with $\mathcal{M}$ and $\mathcal{N}$ self-adjoint differential operators defined by

$$\mathcal{M}[W] := \left(A(\rho)W''\right)'' + \left(B(\rho)W'\right)' + C(\rho)W, \tag{19}$$

$$\mathcal{N}[W] := \left(P(\rho)W'\right)' + Q(\rho)W, \tag{20}$$

where

$$A(\rho) := \rho, \qquad B(\rho) := -\frac{2n^2+1}{\rho}, \qquad C(\rho) := \frac{n^2(n^2-4)}{\rho^3},$$

and

$$P(\rho) := \rho\left(-1+\frac{1}{\rho^2}\right), \qquad Q(\rho) := \frac{n^2}{\rho}\left(1+\frac{1}{\rho^2}\right).$$

Such generalised eigenvalue problems are discussed very scarcely in the solid-mechanics literature; the only exception that we are aware of is the excellent book by Collatz [30] which contains generalisations of Courant's maximum-minimum principle and various comparison theorems that lead to upper and lower bounds for Λ. Unfortunately, the theory developed in that reference is not applicable in our context as it requires some rather stringent conditions on $\mathcal{M}$ and $\mathcal{N}$; this will be explained below. First, it must be pointed out that since in (18) the order of differentiation on the right-hand side is strictly less than the order of differentiation on the left-hand side, the spectrum of a boundary eigenvalue problem associated with such a differential equation is discrete and all eigenvalues have finite algebraic multiplicity (for instance, see [31]).

The Rayleigh quotient for (18), denoted by $\mathcal{R}[W]$ here, can be found in the usual way by multiplying the equation by W and integrating the resulting equality from η to 1. On making use of the integration by parts formula and the kinematic boundary condition $W(\eta) = 0$, it is found that

$$\mathcal{R}[W] = \frac{\int_\eta^1 W(\rho)\mathcal{M}[W](\rho)\,\mathrm{d}\rho}{\int_\eta^1 Q(\rho)W^2(\rho)\,\mathrm{d}\rho - \int_\eta^1 P(\rho)W'^2(\rho)\,\mathrm{d}\rho}. \tag{21}$$

Since $P \geq 0$ and $Q > 0$, the denominator of this quotient can become very close to zero under certain circumstances, and this is indeed the case as it is suggested by the numerical results shown in Figure 3. Also, an arbitrary choice of test functions in either the Rayleigh–Ritz or Galerkin methods can lead to a zero denominator and this seems to be the situation in [6] (this zero denominator does occur for values of η outside the range shown in Figure 4). It should be noted that most methods for approximating eigenvalues [22, pp. 401–413], [30], [32, pp. 397–465], [33] of problems of the type (18) are based on the positive definiteness of the

quadratic functional that appears in the denominator of (21). This condition is obviously violated in the present context, the proof of this fact following next. To this end, we define the function $\varphi : (0, 1] \to \mathbb{R}$ by

$$\varphi(x) := n^2 \int_x^1 \frac{1}{\rho}\left(1+\frac{1}{\rho^2}\right) W^2(\rho)\,\mathrm{d}\rho - \int_x^1 \left(\frac{1}{\rho}-\rho\right) W'^2(\rho)\,\mathrm{d}\rho, \tag{22}$$

where $W(\rho)$ is any smooth function (left unspecified for the time being), and our aim is to show that one can always find two distinct numbers, say $x_1,\ x_2 \in (0, 1)$ (depending on n), such that $\varphi(x_1)\varphi(x_2) \le 0$. This will ensure the existence of at least one zero for φ, and hence for the denominator of the Rayleigh quotient (21).

Our first claim is that $\varphi(1/n) \ge 0$. Indeed,

$$\begin{aligned}\varphi\left(\frac{1}{n}\right) &= n^2 \int_{1/n}^1 \frac{1}{\rho}\left(1+\frac{1}{\rho^2}\right) W^2(\rho)\,\mathrm{d}\rho - \int_{1/n}^1 \left(\frac{1}{\rho}-\rho\right) W'^2(\rho)\,\mathrm{d}\rho \\ &\ge 2n^2 \int_{1/n}^1 W^2(\rho)\,\mathrm{d}\rho - \left(n-\frac{1}{n}\right)\int_{1/n}^1 W'^2(\rho)\,\mathrm{d}\rho,\end{aligned} \tag{23}$$

and the right-hand side of (23) is positive as can easily be inferred by considering a new function $\psi : (0, 1] \to \mathbb{R}$,

$$\psi(x) := \int_x^1 W^2(\rho)\,\mathrm{d}\rho - \frac{1}{2x}\left(1-\frac{1}{x^2}\right)\int_x^1 W'^2(\rho)\,\mathrm{d}\rho.$$

Clearly, this function is continuously differentiable, and a simple exercise shows that

$$\psi'(x) = -W^2(x) + \frac{1}{2x}\left(1-\frac{1}{x^2}\right) W'^2(x) + \frac{1}{2x^2}\left(1-\frac{3}{x^2}\right)\int_x^1 W'^2(\rho)\,\mathrm{d}\rho < 0$$

if $0 < x \le 1$, *i.e.*, ψ is a decreasing function on (0, 1], and hence $\psi(x) \ge \psi(1) = 0$. By setting $x := 1/n$ the positivity of the expression mentioned above is recovered.

Consider now $\varphi(x)$ when $x \approx 1$ and $W(\rho)$ satisfies the kinematic boundary condition (11a); thus, we should require that $W(x) = 0$. In this case we can approximate the expression of this function by taking into account that $W(\rho) = \alpha(\rho - x) + o(\rho - x)$ and $W'(\rho) = \alpha + o(1)$ for $x \le \rho \le 1$ when $x \to 1$, where $\alpha := W'(1)$. Together with (22) these approximations lead to

$$\begin{aligned}\varphi(x) &= \alpha^2\left[n^2\int_x^1 \frac{1}{\rho}\left(1+\frac{1}{\rho^2}\right)(\rho-x)^2\,\mathrm{d}\rho - \int_x^1\left(\frac{1}{\rho}-\rho\right)\mathrm{d}\rho\right] + o\left((1-x)^2\right) \\ &= \alpha^2\left[n^2(x^2 - x^2\log x - \log x - 1) - \left(\frac{x^2}{2} - \log x - \frac{1}{2}\right)\right] + o\left((1-x)^2\right),\end{aligned}$$

as $x \to 1$. The existence of $x_2 \in (0, 1)$ such that $\varphi(x_2) \le 0$ will follow once we show that the expression in the square bracket is negative for $1 - x$ arbitrarily close to zero; the reason for this being that the square bracket is an $o(1-x)$ term but not an $o((1-x)^2)$ one. With the substitution $y := x^2$ we note that this requirement amounts to

$$\log y > \frac{y(2n^2-1) - (2n^2-1)}{yn^2 + (n^2-1)}, \tag{24}$$

for some $y \in (0, 1)$, which in turn suggests considering $h : (0, 1] \to \mathbb{R}$ defined by

$$h(y) := \log y - \frac{(2n^2-1)(y-1)}{yn^2 + (n^2-1)}.$$

Table 1. Approximate values of $\eta^{(n)}$ as given by (25).

n	$\eta^{(n)}$	$\overline{\eta}^{(n)}$	$\lvert\eta^{(n)} - \overline{\eta}^{(n)}\rvert$
2	0·6479625332	0·7500000000	0·1020374668
3	0·8379153795	0·8888888888	0·0509735093
4	0·9077060613	0·9375000000	0·0297939387
5	0·9405976616	0·9600000000	0·0194023384
6	0·9586218956	0·9722222222	0·0136003266
7	0·9695436254	0·9795918367	0·0100482113
8	0·9766539110	0·9843750000	0·0077210890
9	0·9815385674	0·9876543209	0·0061157535
10	0·9850374627	0·9900000000	0·0049625373
11	0·9876288977	0·9917355371	0·0041066394
12	0·9896014053	0·9930555555	0·0034541502
13	0·9911373824	0·9940828402	0·0029454578

The derivative of this function is

$$h'(y) = \frac{y^2 n^4 - y\left[2n^2(n^2-1)+1\right] + (n^2-1)^2}{(yn^2+n^2-1)^2},$$

and solving the equation $h'(y) = 0$, we find

$$y_* = \left(1 - \frac{1}{n^2}\right)^2 \qquad \text{and} \qquad y_{**} = 1,$$

the critical points of h. Since $h'(y) < 0$ for $y \in (y_*, y_{**})$, the inequality (24) follows at once for y in this range.

To summarise, we have shown that for each given $n \geq 2$ one can find $\eta^{(n)} \in (0, 1)$ such that the denominator of the Rayleigh quotient (21) becomes zero when $\eta = \eta^{(n)}$. There is compelling numerical evidence that an even stronger result holds, namely, $\eta^{(n)}$ is unique and $\Lambda(\eta, n) \to \infty$ as $\eta \to \eta^{(n)}$ but we have not been able to justify this rigorously. It might be worth pointing out that very good approximations for $\eta^{(n)}$ can be obtained by setting to zero the aforementioned denominator, and using $W(\rho) := \rho - \eta$ as an assumed form for the eigenmodes of (10)–(11); the transcendental equation to be solved is then found to be

$$\eta^2\left(n^2 - \frac{1}{2}\right) - n^2\eta^2 \log\eta + (1-n^2)\log\eta - \left(n^2 - \frac{1}{2}\right) = 0, \tag{25}$$

and its solutions for $n = 2, \ldots, 13$ are recorded in Table 1. The arguments presented above and the numerical experiments suggest that $\eta^{(n)} \approx \overline{\eta}^{(n)}$ for $n \geq 4$, where $\overline{\eta}^{(n)} = 1 - 1/n^2$ (see the same table for further details).

The comparisons between these "blow-up" values of η and the response curves obtained with the help of the compound matrix method are shown in Figure 8. The vertical dashed lines correspond to the equations $\eta = \eta^{(n)}$ and the continuous curves are the ones already presented in the previous section (see Figure 3). In spite of the many approximations made, it turns out that the values predicted by (25) mirror closely the vertical asymptotes of the response curves; this holds true even in the cases $n = 2$ and $n = 3$ which, strictly speaking, lie outside the range of validity of the approximation made. One of the reasons for such a success is due to the fact that the eigenmodes of the original boundary-value problem are "almost" straight lines passing through $x = \eta$.

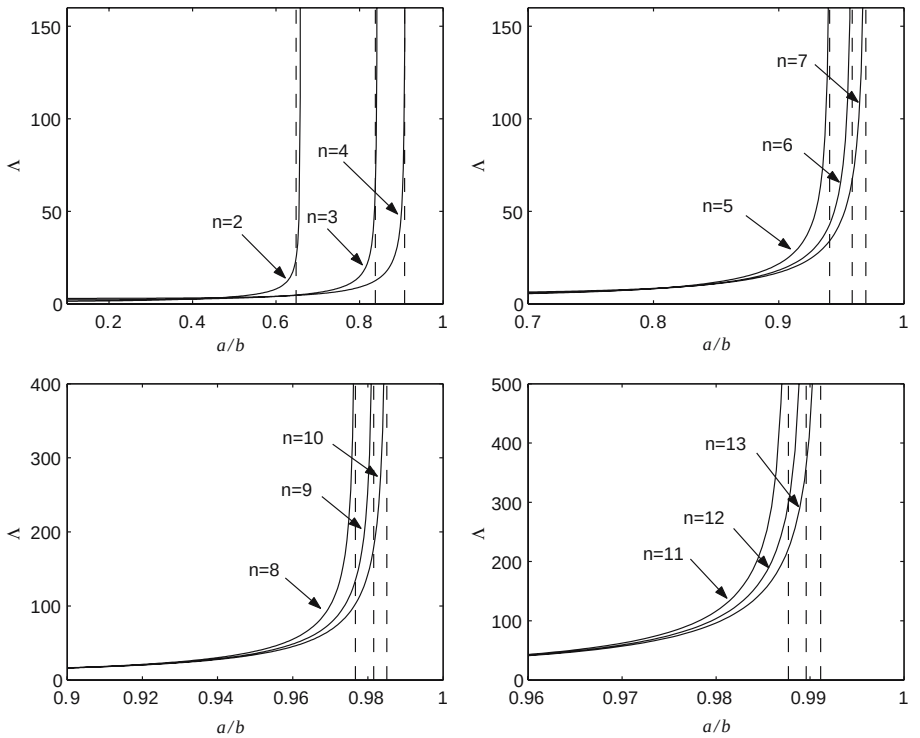

Figure 8. A close look at the blow-up behaviour of the eigenvalues $\Lambda(\eta, n)$ for $n = 2, \ldots, 13$; the vertical dashed lines correspond to the approximate solutions of the equation obtained by setting to zero the denominator of the Rayleigh quotient (see (25)), while the continuous curves are those already presented in Figure 3.

Next, we show that it is possible to extract some useful information about the eigenvalues of (18). We start from the observation that the Rayleigh quotient can be written more conveniently with the help of the original boundary conditions (11) and successive integration by parts, as

$$\mathcal{R}[W] = \frac{I_1 + (2n^2+1)I_2 + n^2(n^2-4)I_3 + K}{n^2 I_4 - I_5}, \tag{26}$$

where

$$I_1 := \int_\eta^1 \rho W''^2 \,\mathrm{d}\rho, \qquad I_2 := \int_\eta^1 \frac{W'^2}{\rho}\,\mathrm{d}\rho, \qquad I_3 := \int_\eta^1 \frac{W^2}{\rho^3}\,\mathrm{d}\rho, \tag{27a}$$

$$I_4 := \int_\eta^1 \left(1+\frac{1}{\rho^2}\right)\frac{W^2}{\rho}\,\mathrm{d}\rho, \qquad I_5 := \int_\eta^1 \rho\left(-1+\frac{1}{\rho^2}\right) W'^2\,\mathrm{d}\rho, \tag{27b}$$

and

$$K := -n^2(3-\nu)W^2(1) - 2\nu n^2 W(1)W'(1) + \nu\left[W'^2(1) - W'^2(\eta)\right].$$

Without loss of generality, we shall normalise the eigenmodes of our eigenvalue problem by the condition

$$\int_\eta^1 \rho W''^2\,\mathrm{d}\rho + \int_\eta^1 \frac{W'^2}{\rho}\,\mathrm{d}\rho + \int_\eta^1 \frac{W^2}{\rho^3}\,\mathrm{d}\rho = 1. \tag{28}$$

Since the coefficients of (10) are analytic functions in $[\eta, 1]$ when $-\infty < \Lambda < \infty$ is regarded as a parameter, the solutions of this equation are well-behaved functions, in particular W, W', W'' are continuous; hence, these functions are bounded and the integrals in (28) are finite for $0 < \eta < \eta^{(n)}$. Obviously, the normalised solutions satisfy $I_j = \mathcal{O}(1)$ for $j = 2, \ldots, 5$ as $n \to \infty$. We are going to see that $W^2(1)$, $W(1)W'(1)$ and $W'^2(1) - W'^2(\eta)$ enjoy the same property. The justification of this assertion follows easily by the application of the Schwarz inequality for integrals. Letting $f(\rho) := \sqrt{\rho}\, W''(\rho)$ and $g(\rho) := W'(\rho)/\sqrt{\rho}$, we get

$$\left| \int_\eta^1 f(\rho) g(\rho)\, \mathrm{d}\rho \right| \le \left(\int_\eta^1 f^2(\rho)\, \mathrm{d}\rho \right)^{1/2} \left(\int_\eta^1 g^2(\rho)\, \mathrm{d}\rho \right)^{1/2} = \sqrt{I_1 I_2} \le \frac{1}{2}(I_1 + I_2) \le 1,$$

which together with

$$\int_\eta^1 f(\rho) g(\rho)\, \mathrm{d}\rho = \int_\eta^1 W''(\rho) W'(\rho)\, \mathrm{d}\rho = \frac{1}{2}\left[W'^2(1) - W'^2(\eta) \right]$$

shows that $W'^2(1) - W'^2(\eta) = \mathcal{O}(1)$ as $n \to \infty$. A similar calculation, this time with $f(\rho) := \sqrt{\rho}\, W(\rho)$ and the same $g(\rho)$ as above, indicates that $W^2(1) = \mathcal{O}(1)$ as $n \to \infty$. Finally,

$$W(1)W'(1) = \int_\eta^1 W'^2(\rho)\, \mathrm{d}\rho + \int_\eta^1 W(\rho) W''(\rho)\, \mathrm{d}\rho,$$

and each integral in this identity can be shown to be bounded independently of n; the first one follows from the fact that $0 < I_2 \le 1$ and the second one requires the application of the Schwarz inequality again. In conclusion, $W(1)W'(1) = \mathcal{O}(1)$ as $n \to \infty$.

Assuming now that $n \gg 1$ and $0 < \eta \ll \eta^{(n)}$, it can be deduced from (26) that

$$\Lambda^2 \approx \left(\frac{I_3}{I_4} \right) n^2. \tag{29}$$

Using elementary inequalities, it can be shown that $2 \le I_4/I_3 \le \eta^3 + 1$ which together with (29) results in

$$\Lambda = \mathcal{O}(n) \qquad \text{or} \qquad \Lambda = \xi n, \qquad \text{with} \quad \frac{1}{\sqrt{2}} \le \xi \le \frac{1}{\sqrt{\eta^3 + 1}}. \tag{30}$$

Strictly speaking this result is valid for $n \gg 1$ and $\eta \ll \eta^{(n)}$, but as we shall shortly see, its limit of validity is far more general. To this end, comparisons between the above estimates and our numerical runs for the problem (10)–(11) are summarised in Table 2, where Λ_{num} signifies the lowest positive eigenvalue of this problem as obtained by numerical integration (see Section 3). We have considered a sample of both relatively small and large representative values of n (10, 30, 50, and 70, respectively) for $\eta \in \{0{\cdot}1, 0{\cdot}3, 0{\cdot}5\}$, and it seems that our estimates are fairly robust.

When $n \gg 1$ and $\eta \approx \eta^{(n)}$ an estimate similar to (30) seems to be out of hand, mainly because of the blow-up behaviour of the eigenvalues Λ. Nevertheless, in this regime one could use the Rayleigh quotient (26) together with the approximation $W(\rho) := \rho - \eta$, and this leads to quite accurate results. We record below the expression of the eigenvalues obtained in this way

$$\Lambda^2 = \frac{\alpha_1 n^4 + \alpha_2 n^2 + \alpha_3}{\beta_1 n^2 + \beta_2}, \tag{31}$$

Table 2. A comparison between the lower/upper bounds for Λ given by (30), and the corresponding values obtained by numerical integration of (10)–(11).

n	η	Λ_{num}	$\Lambda_{\min} := n/\sqrt{2}$	$\Lambda_{\max} := n/\sqrt{\eta^3+1}$
70	0·1	50·6964	49·4975	69·9650
–	0·3	50·6964	49·4975	69·0737
–	0·5	50·6964	49·4975	65·9966
50	0·1	36·4372	35·3553	49·9750
–	0·3	36·4372	35·3553	49·3384
–	0·5	36·4372	35·3553	47·1405
30	0·1	22·1145	21·2132	29·9850
–	0·3	22·1145	21·2132	29·6030
–	0·5	22·1146	21·2132	28·2843
10	0·1	7·59053	7·07106	9·99501
–	0·3	7·59177	7·07106	9·86772
–	0·5	7·64527	7·07106	9·42810

where

$$\alpha_1 := -\frac{\eta^2}{2} + 2\eta - \log\eta - \frac{3}{2}, \quad \alpha_2 := 2\eta^2 - 8\eta - (3-\nu)(1-\eta)^2 - 2\nu(1-\eta) + 2\log\eta + 6,$$

$$\alpha_3 := -\log\eta, \qquad \beta_1 := \eta^2 - \eta^2\log\eta - \log\eta - 1, \qquad \beta_2 := -\frac{\eta^2}{2} + \log\eta + \frac{1}{2}.$$

Figure 9 contains the comparison of (31) with the numerical data. In order to stress the dramatic improvement displayed by such a simple formula, the same scaling and axis limits as in Figure 4 have been used. The agreement with the numerical results is exceptionally good when $a/b \equiv \eta > 0{\cdot}7$ for all the curves included, although n is relatively small; the same holds true for larger values of the mode number but for the sake of brevity these results are not shown here. This unexpected outcome should come as no surprise if one remembers that the only kinematic boundary condition in (11) is the first one, which the test function used in (31) incidentally satisfies.

We note in passing a related effort, the original work of Fu [26] who reports some asymptotic approximations for the response curves in the problem of buckling of a spherical shell subjected to hydrostatic pressure. His idea was to use the mode number n as a large perturbation parameter in conjunction with the classical WKB method. Although there is a great deal of similarity between his Figure 1 and our Figure 3, there are some subtle differences which make that approach unfruitful in the present context. One of them is the fact that, unlike in [26], for our problem Λ is at least $\mathcal{O}(n)$ for $n \gg 1$, and this leads to some ambiguity as to the right expansion for the eigenvalues. Moreover, even in the simple case $\Lambda = \mathcal{O}(n)$, the expressions of the roots for the characteristic equation of (10) look rather unpromising. Hence, the analytical calculations become unmanageable right from the outset. Also, in that work the switching process between C_n and C_{n+1} (see Section 3) is rather different, in the sense that for $\eta \approx 1$ the critical eigenvalues lie mostly on C_n, for some large $n \in \mathbb{N}$, and there is no blow-up in the response curves.

In closing this section, it is worth mentioning a different, more rigorous approach for obtaining approximations to the eigenvalues of (18) for the case when $\eta \approx \eta^{(n)}$ but no restrictions are placed on the mode number. Such an alternative is based on the close resemblance of this problem with the Orr–Sommerfeld equation (see [23, pp. 153–245] for a comprehensive

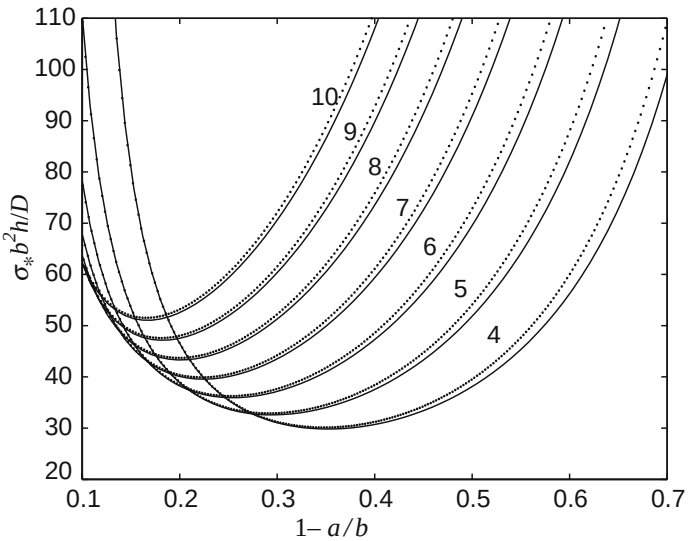

Figure 9. Comparisons between the response curves obtained by numerical integration (continuous line), and the approximation (31) (dotted line) for $n=4, \ldots, 10$; the numbers by each pair of curves indicate the corresponding value of the mode number n.

discussion of this topic). Regarding Λ as a large perturbation parameter and trying to apply the classical WKB method, one finds that the characteristic equation of the differential equation (10) is

$$p^4 - p^2\left(-1+\frac{1}{\rho^2}\right)=0,$$

which has two repetead roots, $p_1=p_2\equiv 0$, and two real distinct ones, $p_{3,4}=\pm\sqrt{1/\rho^2-1}$ which coalesce when $\rho=1$. In the terminology of differential equations, this means that $\rho=1$ is a *turning point* for (10). The four linearly independent solutions away from the turning point can be constructed in the usual fashion [23, pp. 164–180], although the presence of a repeated root does cause a slight complication. Unfortunately, these solutions fail near $\rho=1$, and hence in the vicinity of this point we need to derive a different set of four linearly independent solutions that ultimately have to be matched to the previously found set. Within this context, the so-called inner problem for (10) can be found by using a local stretching transformation of the form $\zeta := \Lambda^\gamma(1/\rho-1)$, where $\gamma>0$ is to be fixed by the usual balancing arguments. Carrying out the appropriate calculations, it is found that $\gamma=2/3$ and the inner equation has the form

$$\frac{\mathrm{d}^4\widehat{W}}{\mathrm{d}\zeta^4}-2\zeta\frac{\mathrm{d}^2\widehat{W}}{\mathrm{d}\zeta^2}+2\frac{\mathrm{d}\widehat{W}}{\mathrm{d}\zeta}=0,$$

where $\widehat{W}(\zeta) := W\left((\zeta/\Lambda^{2/3}+1)^{-1}\right)$. This problem can be solved by the method of Laplace integrals and it is reminiscent of a similar equation obtained by Langer [34] in the study of some hydrodynamical problems. In light of the excellent agreement between our approximations and the numerics, we have not considered imperative to pursue this line of attack here but we shall report these results elsewhere.

5. Conclusions

In this study we have investigated an eigenvalue problem for the elastic instabilities of an annular plate in tension on its inner edge and stress-free on the outer one. This configuration can serve as a simplified model for the wrinkling instabilities encountered in deep-drawing manufacturing processes.

The thrust of the work reported has been twofold. Firstly, we have explored the accuracy of some approximate solutions proposed in the literature, and have performed a numerical study of the dependence of the lowest eigenvalue on the critical mode number and η, the ratio of the inner and, respectively, the outer radii of the plate. Our results suggest that the naive application of the Galerkin method leads to unsatisfactory results for this problem, and the cause of this disagreement is rooted in the lack of positive-definiteness of the Rayleigh quotient (*cf.* [30, Section 15.1]), and the poor choice of test function. Secondly, some mathematical arguments have been employed to consolidate and amplify our understanding of the behaviour of the eigenvalues for this problem. In particular, an interesting feature that emerged in the course of our work is the blow-up behaviour of the eigenvalues, $\Lambda \equiv \Lambda(\eta, n)$, in the governing boundary-value problem describing the wrinkling instability. We have been able to provide both numerical and analytical evidence which suggests that $\Lambda(\eta, n) \to \infty$ as $\eta \to \eta^{(n)}$, where $\eta^{(n)} \in (0, 1)$ is a sequence of numbers such that $\eta^{(n)} \to 1$ as $n \to \infty$. A simple approximation for these blow-up points has also been given. We remark in passing that, for the eigenvalue problem describing the buckling of annular plates in shearing, it is very likely that a similar blow-up occurs (see [35, Figure 2]), and this aspect will be analysed in the future. In that case, the pre-buckling solution can be calculated explicitly from (1) with an appropriate set of boundary conditions, and the bifurcation equation (6) can be easily modified to include the pre-buckling shear stress. There is an extra complication, though, and this is due to the modified form of the normal mode solution (9), which has to be replaced by $w(\rho, \theta) = W_1(\rho)\cos(n\theta) + W_2(\rho)\sin(n\theta)$. The upshot of this change in the form of $w(\rho, \theta)$ is that (10) will become a complex differential equation for the complex-valued function $W(\rho) := W_1(\rho) + \mathrm{i}\, W_2(\rho)$.

In a related paper [17], we have investigated the wrinkling instability of an annular plate corresponding to the scenario outlined in Figure 2. The motivation behind that work was somewhat different from the one presented herein, but the analysis was conducted upon an equation similar to (10). By exploiting the presence of a natural large parameter and using a WKB analysis, we have been able to show in that case that the wrinkling instability can be described by a reduced second-order boundary-value problem. Although such a large parameter is absent from (10), the analysis of the previous section shows that Λ can act as a substitute when η is sufficiently close to $\eta^{(n)}$. Within that regime, there is scope to extend the asymptotic analysis of [17] to the present problem, and this is the subject of a forthcoming study.

Finally, in future works we shall assess the validity of the Galerkin approximation for the elasto-plastic counterpart of the wrinkling problem discussed in this paper (see [36] as well).

Acknowledgements

The first author was supported by The Nuffield Foundation (UK) through a Newly Appointed Lecturers Award. We are grateful for the comments of the referees which have helped to improve the presentation of this paper.

References

1. S.P. Timoshenko, *History of Strength of Materials*. New York: Dover Publications (1988) 452 pp.
2. M. Potier-Ferry, Foundations of elastic post-buckling theory. In: J. Arbocz *et al.* (ed.), *Buckling and Post-buckling*. Berlin: Springer-Verlag (1987) pp. 1–79.
3. W. Johnson and P.B. Mellor, *Engineering Plasticity*. London: van Nostrand Reinhold (1978) 646 pp.
4. R.A.C. Slater, *Engineering Plasticity: Theory and Application to Metal Forming Processes*. London: McMillan Press Ltd. (1977) 422 pp.
5. B.W. Senior, Flange wrinkling in deep-drawing operations. *J. Mech. Phys. Solids* (1956) 235–246.
6. T.X. Yu and L.C. Zhang, The elastic wrinkling of an annular plate under uniform tension on its inner edge. *Int. J. Mech. Sci.* 28 (1986) 729–737.
7. T.X. Yu and W. Johnson, The buckling of annular plates in relation to the deep-drawing process. *Int. J. Mech. Sci.* 24 (1982) 175–188.
8. J.W. Geckler, Plastiche knicken der wandung von hohlzylindern und einige andern faltungserscheinungen. *ZAMM* 8 (1928) 341–352.
9. E.H. Mansfield, On the buckling of an annular plate. *Quart. J. Appl. Math.* 13 (1960) 16–23.
10. N.A. Alfutov, *Stability of Elastic Structures*. Berlin: Springer-Verlag (2000) 337 pp.
11. N. Friedl, F.G. Rammerstorfer and F.D. Fischer, Buckling of stretched strips. *Comput. Struct.* 78 (2000) 185–190.
12. E. Cerda and L. Mahadevan, Geometry and physics of wrinkling. *Phys. Rev. Lett.* 90 (2003) 1–4.
13. E. Cerda, Mechanics of scars. *Journal of Biomechanics* 15 (2005) 117–126.
14. K. Burton and D.L. Taylor, Traction forces of cytokinesis measured using optically modified elastic substrata. *Nature* 385 (1997) 450–454.
15. A.K. Harris, P. Wild and D. Stopak, Sillicone rubber substrata: a new wrinkle in cell locomotion. *Science* 208 (1980) 177–179.
16. J.C. Géminard, R. Bernal and F. Melo, Wrinkle formations in axis-symmetrically stretched membranes. *Eur. Phys. J. E* 15 (2004) 117–126.
17. C.D. Coman and D.M. Haughton, Localised wrinkling instabilities in radially stretched annular thin films. *Acta Mechanica* (to appear in 2006).
18. A. Gilabert, P. Sibillot, D. Sornette, C. Vanneste, D. Maugis and F. Muttin, Buckling instability and patterns around holes or cracks in thin plates under a tensile load. *Eur. J. Mech., A/Solids* 11 (1992) 65–89.
19. W.S. Slaughter, *The Linearized Theory of Elasticity*. Boston: Birkhäuser (2002) 543 pp.
20. D.O. Brush and B.O. Almroth, *Buckling of Bars, Plates, and Shells*. New York: McGraw-Hill (1975) 379 pp.
21. P.S. Bulson, *The Stability of Flat Plates*. London: Chatto & Windus (1970) 470 pp.
22. C.L. Dym and I.H. Shames, *Solid Mechanics: A Variational Approach*. New York: McGraw-Hill (1973) 536 pp.
23. P. Drazin and W. Reid, *Hydrodynamic Stability*. Cambridge: Cambridge University Press (1981) 525 pp.
24. D.M. Haughton and A. Orr, On the eversion of compressible elastic cylinders. *Int. J. Solids Structures* 34 (1997) 1893–1914.
25. D.M. Haughton, Flexure and compression of incompressible elastic plates. *Int. J. Engng. Sci.* 37 (1999) 1693–1708.
26. Y.B. Fu, Some asymptotic results concerning the buckling of a spherical shell of arbitrary thickness. *Int. J. Non-Linear Mechanics* 33 (1998) 1111–1122.
27. E.J. Doedel, A.R. Champneys, T.F. Fairgrieve, Y.A. Kuznetsov, B. Sandstede and X. Wang, AUTO97: continuation and bifurcation software for ordinary differential equations. Available via anonymous from fttp://ftp.cs.concordia.ca/pub/doedel/auto, 1997.
28. M.A. Naimark, *Elementary Theory of Linear Differential Operators*. London: George G. Harap & Company, Ltd. (1967) 144 pp.
29. E. Chu and Yu Xu, An elastoplastic analysis of flange wrinkling in deep drawing processes. *Int. J. Mech. Sci* 43 (2001) 1421–1440.
30. L. Collatz, *Eigenwertprobleme und Ihre Numerische Behandlung*. New York: Chelsea Publishing Company (1948) 338 pp.
31. E. Kamke, *Differentialgleichungen*, volume 1. Leipzig: Akademische Verlagsgesellschaft Geest & Portig (1969) 666 pp.
32. R. Courant and D. Hilbert, *Methods of Mathematical Physics*, volume 1. New York: Interscience Publishers Inc. (1966) 561 pp.

33. H.F. Weinberger, *Variational Methods for Eigenvalue Approximation*. Philadelphia: Society for Industrial and Applied Mathematics (1974) 160 pp.
34. R.E. Langer, Formal solutions and a related equation for a class of fourth order differential equations of hydrodynamic type. *Trans. Amer. Math. Soc.* 92 (1959) 371–410.
35. C. Chang-jun and L. Xiao-an, Buckling and post-buckling of annular plates in shearing, Part I: Buckling. *Comput. Methods Appl. Mech. Engrg.* 92 (1991) 157–172.
36. L.C. Zhang and T.X. Yu, The plastic wrinkling of an annular plate under uniform tension on its inner edge. *Int. J. Solids Structures* 24 (1988) 497–503.